Multiferroic (Nd,Fe)-doped PbTiO3 ceramics with coexistent ferroelectricity and magnetism at room temperature

Multiferroic (Nd,Fe)-doped PbTiO3 Ceramics with Coexistent Ferroelectricity and Magnetism at Room Temperature (CJ-3:IL05)

F. Craciun[*,1], F. Cordero[1], M. Cernea[2], M. Zaharescu[3], V. Fruth[3], I. Atkinson[3], N. Stanica[3], B. S. Vasile[4], A. Iuga[2], P. Galizia[5] and C. Galassi[5]

[1]Istituto di Struttura della Materia-CNR (ISM-CNR), Area di Ricerca di Roma-Tor Vergata, Via del Fosso del Cavaliere 100, I-00133 Rome, Italy

[2]National Institute of Materials Physics, Atomistilor 405 A, 077125 Bucharest-Magurele, Romania

[3]Institute of Physical Chemistry, Romanian Academy, Spl. Independentei 202, 060021 Bucharest, Romania

[4]Faculty of Applied Chemistry and Material Science, University Politehnica of Bucharest, 1-7 Gh. Polizu Street, Bucharest 011061, Romania

[5]CNR-ISTEC, Istituto di Scienza e Tecnologia dei Materiali Ceramici, via Granarolo 64, I-48018 Faenza, Italy

Abstract: We report the structural, dielectric, elastic, ferroelectric and ferromagnetic properties of multiferroic (Nd, Fe)-doped PbTiO3 perovskite ceramics with composition $(Pb_{0.88}Nd_{0.08})(Ti_{0.94}Fe_{0.4}Mn_{0.02})O_3$, prepared by different solid state reaction methods: the first one based on a single-stage calcination (Method I) and the second based on a double-stage calcination (Method II). Structural, dielectric and anelastic measurements evidenced a double phase transition for samples prepared by Method I, which has been attributed to phase separation. This phase separation has been confirmed also by TEM and HRTEM investigations. Samples prepared by Method II showed a single phase transition from paraelectric to ferroelectric phase. We found coexistent ferroelectric and ferromagnetic properties, also at room-temperature, but only for ceramics prepared by Method II. The crucial role of calcination process for avoiding phase separation and obtaining homogeneous structures with ferroelectric and ferromagnetic order is underlined.

1. **Introduction**

Multiferroics are materials which show simultaneously two or more ferroic order parameters:

ferroelectric, magnetic, elastic etc. Usually the most interesting combination includes the first two order parameters, therefore we will consider these type of materials.

Since many decades, the field of multiferroic materials has been intensively investigated due to the high interest in materials which would allow the simultaneous control of multiple order parameters like multiple state memory elements, spintronic devices, sensors and other multifunctional devices [3-7PCCP]. Single-phase multiferroics with coupled long-range ferroelectricity and magnetism are a subgroup of ferroelectrics. They are distinguished from composite multiferroics, where ferroelectric and magnetic phases are combined at macroscopic level [Fiebig]. The number of naturally occurring single-phase multiferroic materials with coexistent ferroelectricity and magnetism is very small. Well-known examples are BiFeO3, BiMnO3, TbMnO3 [ ].

Generally, multiferroic materials are obtained by doping magnetic materials in order to induce ferroelectric properties [ ]. However these materials show very weak ferroelectric properties. The other way is to substitute magnetic ions in ferroelectric materials with good ferroelectric properties. Many perovskite-like multiferroic compositions have been thus obtained, starting from ferroelectric or relaxor ferroelectric perovskites doped on the B-site with different magnetic ions [10-13PCCP]. Different doping elements have been used to induce magnetic properties in PbTiO3. For example a rare earth *R* magnetic element has been substituted on the A-site and/or one or more transition metal *M* elements have been substituted on the B-site. Thus (Pb,Nd)TiO3, PbFeO3 and Pb(Ti,Fe)O3 have been investigated [JMS, Palkar, Tsuchiya]. We have previously reported preliminary investigations on the ferroelectric and magnetic properties of lead titanate doped with Nd3+ or Sm43+ on the Pb-site and with (Fe3+, Mn4+) on the Ti site [APL, JAP. MD]. The ordering of dopants and the incipient formation of separate phases in $(Pb,Nd)(Ti,Fe,Mn)O_3$ has been investigated [PCCP]. Fe57 Mossbauer spectroscopy was applied with the aim to provide information on the coordination and valence of the iron ions and XPS measurements have been carried out to assess the valence of different cations in the structure, especially of Ti and Fe ions [PCCP].

In this study we investigate the structural, dielectric, elastic, ferroelectric and ferromagnetic properties of perovskite ceramics with composition $(Pb_{0.88}Nd_{0.08})(Ti_{0.94}Fe_{0.4}Mn_{0.02})O_3$ prepared by different solid state reaction methods, evidencing the role of calcination process in avoiding phase separation and obtaining homogeneous structures with ferroelectric and ferromagnetic properties.

2. Experimental

Powders and ceramic samples with composition $(Pb_{0.88}Nd_{0.08})(Ti_{0.94}Fe_{0.4}Mn_{0.02})O_3$, hereafter called N4, have been prepared by standard solid state reaction method and ceramic processing, according to two procedures. The reagent grade component powders have been weighed according to the

composition then mixed in ethylic alcohol using a rotary ball mill for 2 h at 350 rot/min, then they were dried. The powders for the samples prepared according to Method I (hereafter called N4-I) have been subjected to a single calcination process at 950 C for 4h in air. The calcination time has been selected in order to ensure the formation of a pure perovskite phase.

The powders for the samples prepared according to Method II (hereafter called N4-II) have been subjected to a first calcination at 850 ^{o}C for 2 h in air. The calcined powders were again milled, following the same procedure, and subjected to a second calcination at 1050 ^{o}C for 1 h.

After milling and drying of both N4-I and N4-II type powders, disc pellets have been uniaxially pressed and sintered in closed crucibles (sealed with $PbTiO_3$ powder) at 1200 °C for 2 h, up to a final density of about 98%. All the characterizations have been made on samples sintered at this temperature, with the same protocol.

The crystallographic structure was examined by using a Rigaku UltimaIV X-ray diffractometer, in parallel-beam geometry. The Cu Kα1 radiation (wavelength 1.5406 Å) from a Cu tube operating at 40 kV and 30 mA has been used for investigation. Counts were collected from 20° to 80° with a step size of 0.02° and a step time of 10 s. Phase identification and lattice parameters calculation were performed using Rigaku PDXL software connected to ICDD PDF-2 database.

TEM, high resolution TEM (HRTEM) and selected area electron diffraction (SAED) have been employed to investigate the ferroelectric domains and local structure of the samples. TEM specimens have been prepared by ultrasonic drilling of thin sample disks which have been further grinded to a thickness of about 10-20 μm. The samples have been attached to a Mo holder and subjected to ion-beam milling in order to obtain an electron transparent sample. TEM, HRTEM and SAED investigations have been carried out on a Tecnai^{TM} G^2 F30 S-TWIN transmission electron microscope with a line resolution of 1 Å in HRTEM mode.

The morphology of fracture surfaces of the sintered ceramic samples was observed by using a FEI QUANTA INSPECT F microscope.

Samples for electrical measurements have been prepared by polishing sintered discs with a diameter of about 10 mm in order to remove the surface layers and to reduce the thickness to about 0.5 mm. Silver paste electrodes have been applied by screen printing and heating at 700 °C.

The dielectric measurements have been carried out on unpoled samples with an HP4284A LCR meter, by using a four wire probe and an ac driving level of 0.5 V/mm. The frequencies of the driving signal have been 0.2, 1, 10, 100 and 200 kHz. The dielectric permittivity $e = e' - i\,e''$ has been calculated from the measured values of capacitance and loss tan $\delta = e''/e'$.

For temperature dependence measurements, the samples have been placed in a modified Linkam HFS600E-PB4 stage and the measurements were made on heating and cooling at 1-1.5

K/min between 90 K and 780 K.

Samples for anelastic measurements have been cut as bars with length about 40 mm, width about 4 mm and thickness about 0.5 mm. The elastic compliance $s(\omega, T)$ was measured by electrostatically exciting the flexural modes of the bars suspended in vacuum on thin thermocouple wires in correspondence with the nodal lines [30]. In these conditions during the same run it is possible to measure the 1st, 3rd and 5th modes. The data are presented as the real part of the elastic compliance s' and the elastic energy loss $Q^{-1} = s''/s'$.

Ferroelectric hysteresis measurements have been performed at room temperature with a Precision Premier II ferroelectric tester from Radiant Technologies.

The magnetization dependence on magnetic field has been measured at different temperatures between 100 K and 350 K by using a 7410 LakeShore Vibrating Sample Magnetometer (VSM).

3. Results and discussion

3.1. Structural properties

The room temperature XRD patterns for the N4-I and N4-II samples in the angular range $20^0 – 80^0$ are shown in Figure 1. Only peaks corresponding to the perovskite phase ($PbTiO_3$, space group 99, P4mm tetragonal symmetry, PDF card-01-070-4258) are registered in both patterns. Small particles of secondary phases, if present, could broaden the reflection peaks, however the XRD patterns in Figure 1 show rather sharp peaks corresponding to $PbTiO_3$-like structure.

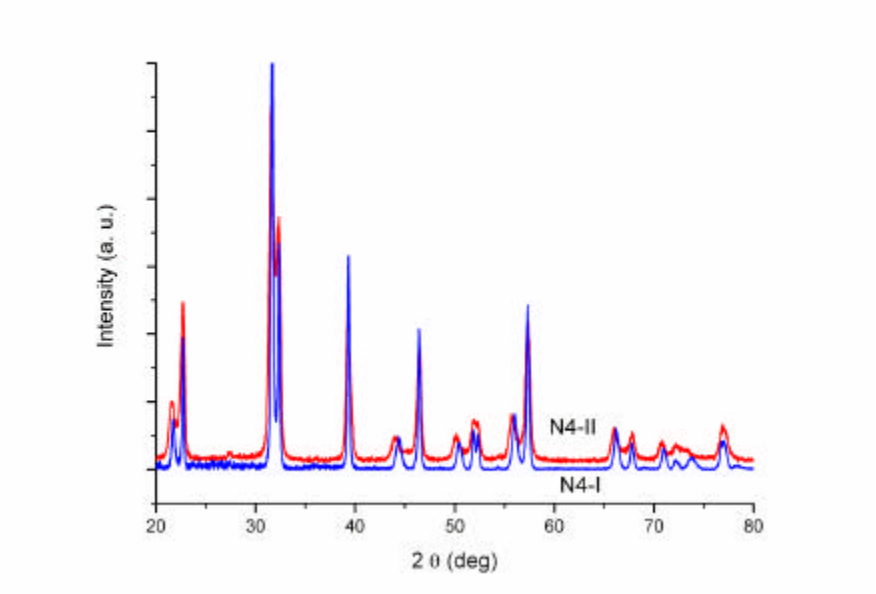

Figure 1. XRD patterns for N4-I and N4-II samples. All the peaks are characteristic for the $PbTiO_3$-like structure (tetragonal symmetry P4mm, PDF card-01-070-4258).

The unit cell parameters obtained from XRD patterns fitting are given in Table 1 for the two types of samples, together with tetragonality and unit cell volume values.

Table 1. Unit cell parameters and tetragonality for the two types of samples.

Sample	a (Å)	c (Å)	c/a	V ($Å^3$)
N4-I	3.9077	4.0815	1.0445	62.325
N4-II	3.8930	4.1050	1.0545	62.285

The departure from the host perovskite structure after substitution of doping elements can be described by the tolerance factor [26 MD]

$$t = \frac{< R_A > + R_O}{\sqrt{2}(< R_B > + R_O)} \qquad (1)$$

where R_A, R_B are the ionic radii of the cations occupying the A- and B-sites of the perovskite structure, while R_O is the ionic radius of the oxygen anion. A tolerance factor t >1 characterizes a good ferroelectric (e. g. for $PbTiO_3$ t ≈ 1.027). In Eq. (1) the average ionic radii of the cations must be used, by taking into account the partial substitutions in A and B-sublattices. By using the average radii $<R_A>$ ≅ 1.4128 Å and $<R_B>$ ≅ 0.604 the calculated value of the tolerance factor for N4 composition is t ≅ 1. Tus due to Nd, Fe and Mn ions substitutions, the tolerance factor decreases and the ferroelectricity and tetragonal anisotropy decreased as well.

From Table 1 it can be observed that the tetragonality of the unit cell is slightly higher for N4-II samples, indicating that the double-stage calcination induces changes at the microscopic level, probably due to the different distribution of substituting elements.

Also the microstructure of the two types of samples looks rather different, as shown in Fig. 2. The fracture surface image corresponding to N4-I type samples shows larger crystallites, with average dimension > 1 μm, while sample N4-II is characterized by submicronic crystallites disposed in very compact aggregates.

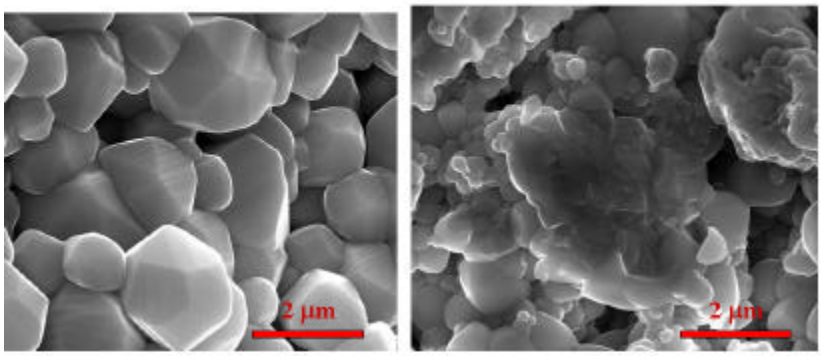

Figure 2. Fracture surface SEM images for the two types of samples.

3.2. Transmission electron microscopy characterization of ferroelectric domains

While TEM images taken on N4-II type samples show almost normal ferroelectric domains with lamellar structure, the images taken on representative regions of N4-I samples demonstrate a great complexity of the domains and walls morphology (Fig. 3 and 4). The usual twinning structures, which occur to relieve the stress during the parelectric-ferroelectric phase transition or to minimize the local depolarization field, are much more distorted, with curved domain boundaries and variable density of domain walls, demonstrating the disturbing effect of magnetic element clusters. In Figure 3 a) 90^0 a-a domain boundaries (lower rectangle) and curved 90^0 a-c domain boundaries, recognizable due to the characteristic fringes (upper ellipsoid) are visible, together with a peculiar nanodomain structure on the left upper angle. Another complex structure is visible in Fig. 3 b) where two systems of 90^0 a-c domain boundaries occur inside a grain, crossing at an angle of about 20^0.

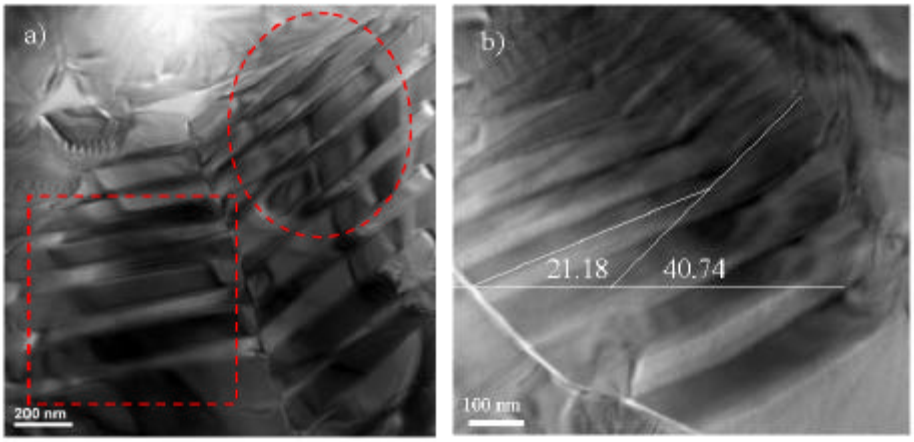

Figure 3 a) TEM image of a zone in N4-I sample showing twin domains with 90^0 a-a domain boundaries (lower rectangle) and curved 90^0 a-c domain boundaries (upper ellipsoid), together with a peculiar nanodomain structure on the left upper angle; b) two different twin systems with 90^0 a-c domain boundaries occuring inside a grain, crossing at an angle of about 20^0.

Figure 4 shows still other peculiar consequences of the existence of inhomogeneities ssociated with magnetic clusters in the samples. In a) a zone apparently free of features near a region populated with ferroelectric twin domains (upper right corner) is shown. When magnified, details in the lower left corner marked by the yelow arrow are clearly visible in Figures 4 b) and c, revealing a "lattice" of nanodomains. In d) the SAED pattern from this zone shows diffraction spot splittings typical for twin domains. In order to understand the cause of this peculiar structure we must turn to the problem of domain generation in ferroelectric perovskites (such as $PbTiO_3$) during the phase transformation from the parent cubic phase to the product tetragonal phase and address the following question: how small an inclusion in the cubic matrix can support a tetragonal phase. This problem is similar to that encountered in ferroelastics [42 MT] where the occurrence of inclusion of martensite phase in the austenite matrix during phase transformation has been considered. For large values of inclusion size the usual twinned domain structure is obtained when the temperature is decreased below the transition temperature. However, for small values of inclusion size it was found that the nucleation of the twinned martensite was not energetically favorable, and on lowering the temperature a heterogeneous structure containing both the parent and product phases

was observed. This is a superposition of twins in crossing directions; thus a checkerboard structure, where parent and product phases alternate, was observed. Actually in our materials formation of twinned domain structures when temperature is decreased from high values to a value near the transition temperature is limited by regions of clustered impurities and in some particular cases formation of such "lattice" structures could be favored. Thus the main cause of the generation of the twinned "lattice" structure is the confinement of the strain field and in some cases this structure can be locked down to the room temperature by the strain field generated by impurity clusters, surviving nearby the usual twin structures (Fig. 4 a).

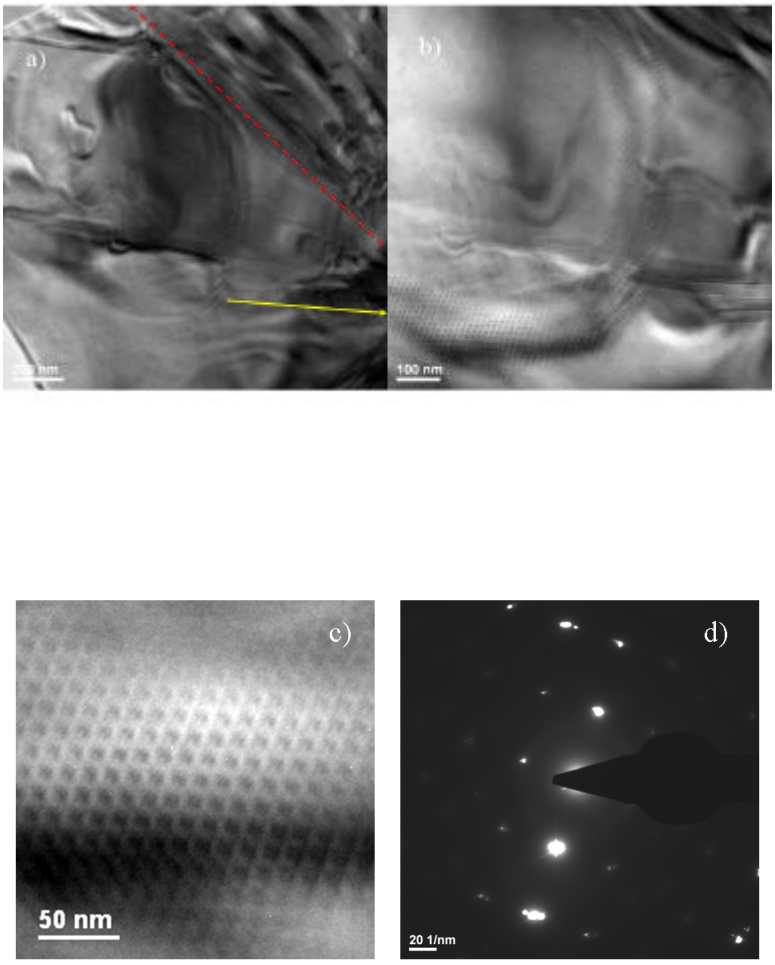

Figure 4 a) TEM image of sample N4-I showing a zone apparently free of features near a region populated with ferroelectric twin domains (upper right corner); b), c) successive magnifications of the lower zone showing a "lattice" of nanodomains, with dimensions below 10 nm; d) SAED pattern from this zone showing diffraction spot splittings typical for twin domains.

Thus the coexistence, in the same region or in neighbouring regions, of ferroelectric domains with approximately regular aspect and of strongly perturbed zones with irregular nanodomains, seems to indicate that N4-I samples are inhomogeneous, with a non-random magnetic ions distributions. Regions with magnetic ion clusters will be strongly perturbed and will show irregular ferroelectric structures, while other regions free of magnetic clusters will show almost normal ferroelectric domains.

3.3. Dielectric properties

Figure 5 shows the results obtained from dielectric spectroscopy measurements at ambient temperature. The frequency variation of dielectric permittivity, dielectric loss tangent and ac conductivity in the frequency range 20 Hz-1 MHz are displayed for the two types of samples.

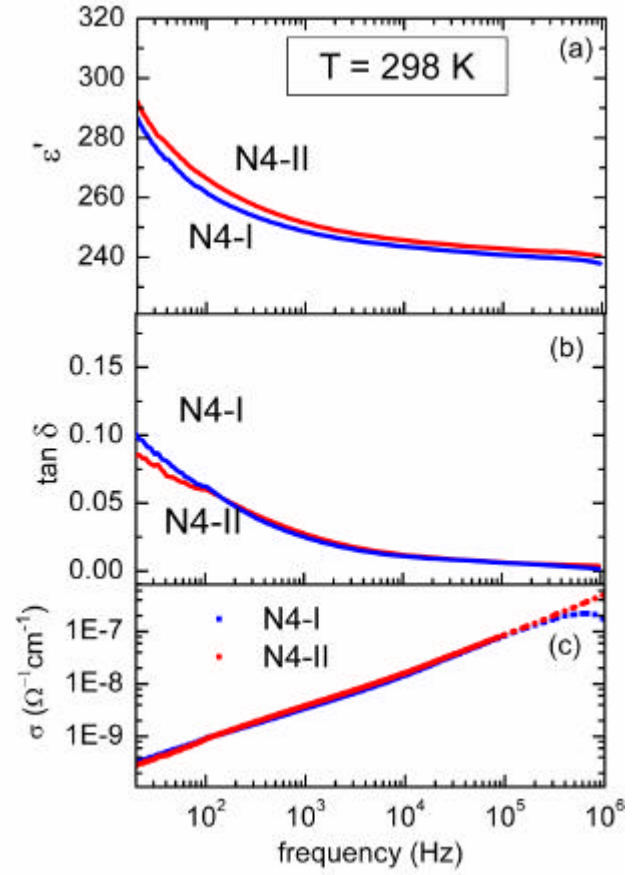

Figure 5. Room temperature frequency variation of dielectric permittivity (a), loss tangent (b) and ac conductivity (c) for N4-I and N4-II samples.

It can be observed that the dielectric constant and loss for both types of samples increase with frequency decreasing, probably due to conductivity. There are only small differences betwen the two types of samples. The dielectric loss tangent preserves a low value (about a few percent) for frequencies above 1 kHz. Both dielectric constant and dielectric loss remain nearly constant in the

frequency range 1 kHz-1 MHz.

The ac conductivity σ at room temperature (Fig. 5 c) shows an almost linear dependence of frequency on log-log scale. This fractional power law dependence seems to be a universal behavior found in many disordered dielectric solids such as ionic conductor glasses, amorphous semiconductors, nonstoichiometric crystals and crystalline materials with many defects [37 Jonscher].

The frequency dependence of the conductivity in disordered solids is described by the Almond-West equation [37]:

$$s(f) \propto f^{n}] \qquad (2)$$

where n is a fractional exponent (0.5<n<1). For the two types of samples n ≈ 0.7.

Figure 6 a) displays the variation with temperature of the real part $e¢$ and loss tangent tan δ of dielectric permittivity, at different frequencies, for N4-I samples. The most remarkable feature is the double peak in the dielectric constant, at about 650 K and 620 K. This is a clear indication that there is a double transition, due to phase separation. As discussed in Ref. [PCCP], on cooling from paraelectric phase, the cubic phase free of magnetic clusters is the first to transform in a tetragonal phase T1, at temperature Tc1. At a slightly lower temperature, Tc2, also the region affected by magnetic clusters transforms in a tetragonal phase T2. The coexistence of these tetragonal phases at room temperature is visualized by TEM, as shown in the previous section.

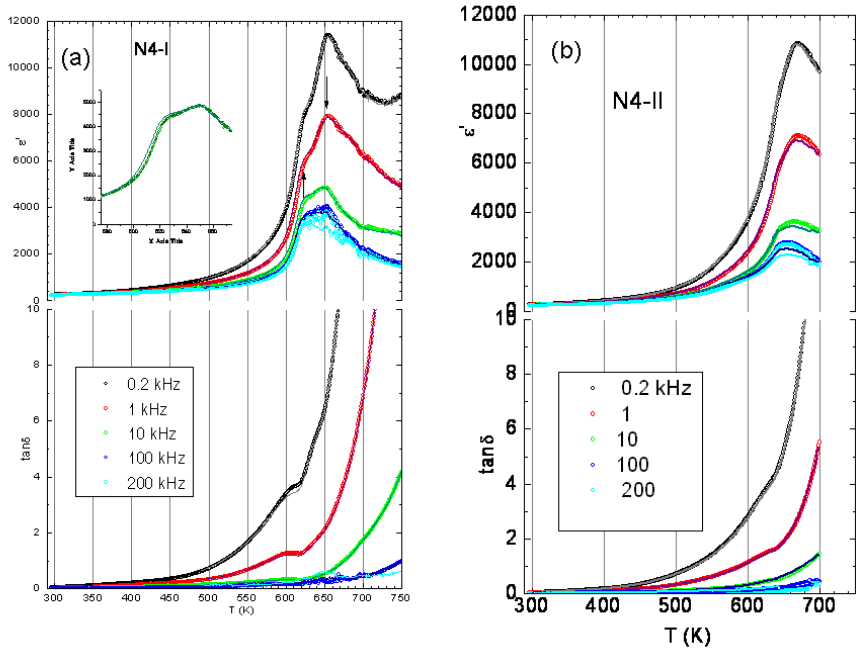

Figure 6 a) Variation with temperature of the real part $e¢$ and loss tangent tan d of dielectric

permittivity, at different frequencies, for N4-I samples. The arrows show the double transition peaks; b) Variation with temperature of the real part ε' and loss tangent tan δ of dielectric permittivity, at different frequencies, for N4-II samples.

Figure 6 b) displays the variation with temperature of the real part *e¢* and loss tangent tan *d* of dielectric permittivity, at different frequencies, for N4-II samples. The dielectric anomaly signals the ferroelectric transition from cubic paraelectric state to tetragonal ferroelectric state. Although broad, the peak signals nevertheless a single phase transition. This indicates that N4-II samples are homogeneous and no phase separation occurs, pointing to a random distribution of magnetic ions in the structure.

The transition peaks for different frequencies are rather broad and show some dispersion due to conductivity, especially at high temperatures and for low frequencies. Also the enhanced losses in the high temperature range and at low frequencies could be explained through the hopping conductivity of oxygen vacancies which is activated at high temperature.

For both types of samples, a decreasing of the critical temperature with respect to that of pure lead titanate (T_c ~ 763 K [35]) is registered. This is consistent with the decrease of the tetragonal c/a ratio, which is an indication of the decreasing of ferroelectricity strength of the lattice.

3.4. Anelastic spectroscopy results

A further confirmation of phase separation in N4-I samples is given by anelastic measurements. In Figure 7 the upper plot represents the elastic compliance normalized to the paraelectric value, while the lower plot represents the inverse of the mechanical quality factor Q^{-1} or mechanical tangent loss.

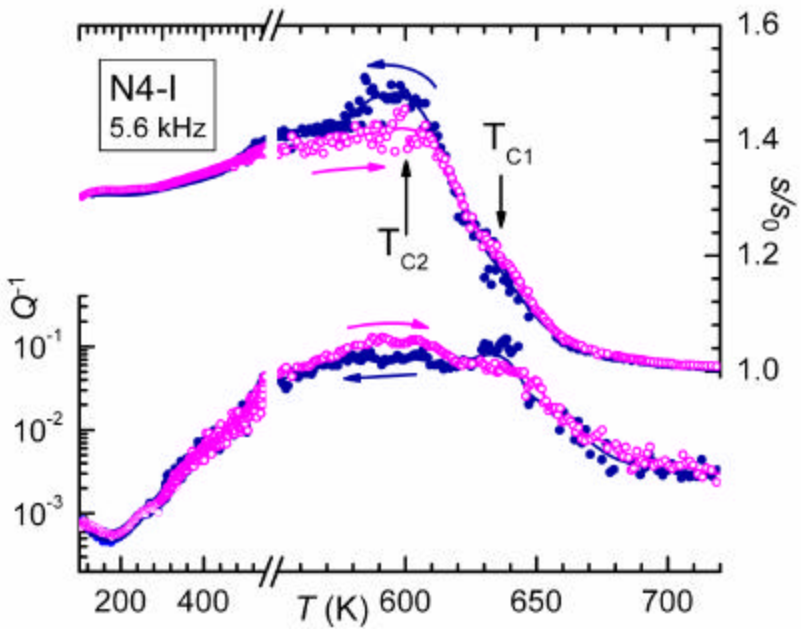

Figure 7. Variation with temperature of the elastic compliance and inverse mechanical quality factor for N4-I samples. The arrows show the double transition peaks.

The step in the elastic compliance is related to the transition between the paraelectric and ferroelectric phase. A remarkable softening occurs at the transition temperature, nearly 1.5 times. It has been shown [59] that this is related to the intrinsic piezoelectric properties of the material.
Another remarkable feature is the double step in the elastic compliance (and, although more shallow, in Q^{-1}) temperatures T_{C1} and T_{C2}. This is a clear indication that there is a double transition. These results are in agreement with dielectric spectroscopy measurements, which evidenced the double transition, at successive temperatures, from the cubic phase free of magnetic clusters to a tetragonal phase T1, and from the cubic phase with magnetic clusters to a tetragonal phase T2.

3.5. Ferroelectric polarization

The ferroelectric polarization has been measured on both types of samples by PUND (positive-up, negative-down) method, in order to eliminate the contribution of leakage currents. By using this method three loops are obtained: i) the total hysteresis loop, including contributions both from ferroelectric processes and losses; b) the non-remanent hysteresis loop, which is a measure of the non-switchable polarization; c) the remanent hysteresis loop, which is the difference between the total and the non-remanent loops, and it is the true measure of the contribution of the switching processes to the polarization. The resultant remanent hysteresis loop has been further corrected, by rescaling the monopolar parts to the lower remanent value, in order to eventually eliminate the step at zero voltage. Hysteresis loops for N4-I and N4-II samples are shown in Figure 8. Although the remanent polarization is much decreased with respect to $PbTiO_3$, the loops are well saturated and the samples show ferroelectric properties. The remanent polarization obtained on N4-II samples is more than two times larger than on N4-I samples, evidencing the disturbing effect of phase separation and magnetic clusters on the ferroelectric properties.

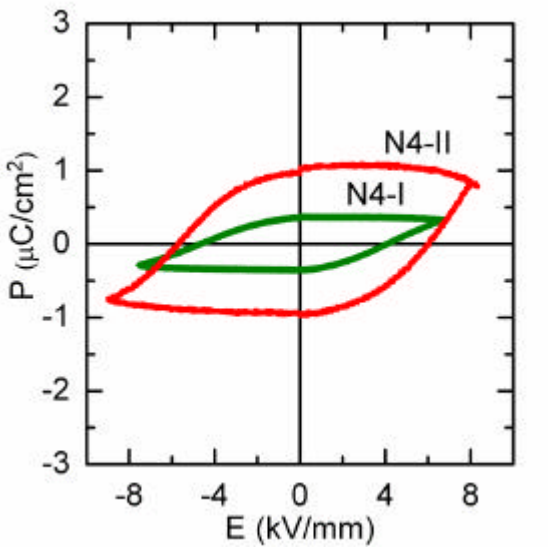

Figure 8. Polarization hysteresis loops obtained by PUND method for N4-I and N4-II samples at room temperature.

3.6. Magnetization measurement results

Figure 9 shows magnetization dependence on the applied magnetic field at T = 100 K and T = 300 K for N4-I (a) and N4-II (b) samples. It can be observed that N4-I samples show paramagnetic behavior. The hysteresys loops are very slim, even at low temperature.

A different behavior is registered for N4-II samples, where a ferromagnetic hysteresis loop, although unsaturated, is measured up to room temperature.

Thus, contrary to what is commonly beleived, an incipient phase separation seems to be detrimental for the magnetic properties. Instead, a random distribution of doping magnetic ions favours the establishing of magnetic order in the samples. This is in agreement with theoretical calculations in Ref. [29 MT] where a comprehensive theoretical study of the effects of magnetic impurity clustering on the magnetization in diluted magnetic systems has been presented, predicting the occurrence of magnetic properties below a certain temperature in systems with random distribution, but not in those with impurity clustering.

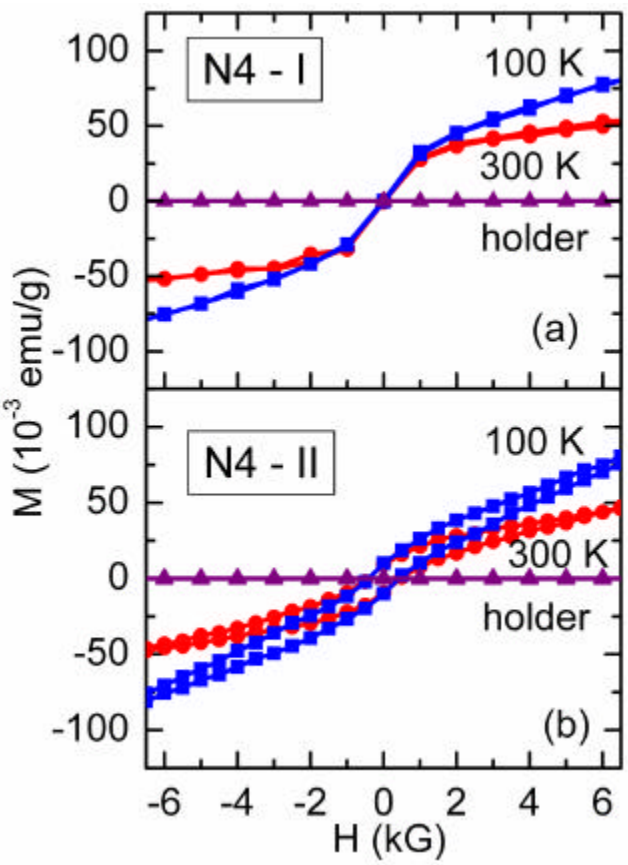

Figure 9. Magnetization dependence on the applied magnetic field at T = 100 K and T = 300 K for N4-I (a) and N4-II (b) samples.

4. Conclusions

In conclusion we have evidenced that the structural, dielectric, elastic, ferroelectric and magnetic properties of multiferroic (Nd, Fe)-doped PbTiO3 perovskite ceramics with composition $(Pb_{0.88}Nd_{0.08})(Ti_{0.94}Fe_{0.4}Mn_{0.02})O_3$, prepared by different solid state reaction methods, are strongly dependent on the solid state processing parameters. Thus samples prepared by a process based on a single-stage calcination (Method I) are less homogeneous than those prepared by employing a double-stage calcination (Method II). Structural, dielectric and anelastic measurements evidenced a double phase transition for samples prepared by Method I, which has been attributed to phase separation. This phase separation has been confirmed also by TEM and HRTEM investigations. Samples prepared by Method II showed a single phase transition from paraelectric to ferroelectric phase. We found coexistent ferroelectric and ferromagnetic properties, also at room-temperature, but only for ceramics prepared by Method II, thus evidencing the crucial role of calcination process for avoiding phase separation and obtaining homogeneous structures with ferroelectric and ferromagnetic order.

Acknowledgments

Financial support from Joint Project CNR – Romanian Academy “Study and Development of Single-Phase Multiferroic Perovskite Ceramic and Thin Films for Multifunctional Devices” is gratefully acknowledged. The authors from the National Institute of Materials Physics-Romania acknowledge the support of the Core program PN09-450, as well as of the European Union and Romanian Government, under POS-CCE project CEUREMAVSU-Nr.01/01.03.2009, allowing the acquisition of the research infrastructure.

References